# FULL PAPER

# The Isoelectronic Replacement of E = P$^+$ and Si in the Trinuclear Organotin−Oxo Clusters [Ph$_2$E(OSn$t$Bu$_2$)$_2$O·$t$Bu$_2$Sn(OH)$_2$]

## Jens Beckmann,*[a] Dainis Dakternieks,[a] Andrew Duthie,[a] Klaus Jurkschat,*[b] Michael Mehring,[b] Cassandra Mitchell,[a] and Markus Schürmann[b]

The trinuclear organotin–oxo cluster [Ph$_2$P(OSn$t$Bu$_2$)$_2$O·$t$Bu$_2$Sn(OH)$_2$][O$_3$SCF$_3$] (**6**), was prepared in good yield by the consecutive reaction of ($t$Bu$_2$SnO)$_3$ with F$_3$CSO$_3$H and Ph$_2$PO$_2$H, and adopts a common tricyclic ESn$_3$O$_3$X$_2$ structural motif with E = P; X = OH, similar to those found in the recently reported species [M(OSn$t$Bu$_2$)$_2$O·$t$Bu$_2$Sn(OH)$_2$] [M = Ph$_2$Si (**1**), Me$_2$Si (**2**), CO (**3**), MesB (**4**)] and [Ph$_2$Si(OSn$t$Bu$_2$)$_2$O·$t$Bu$_2$SnF$_2$] (**5**) where E = Si, C, B and X = OH, F. Compound **6** was characterized by multinuclear NMR spectroscopy, IR spectroscopy, electrospray mass spectro-

metry and single-crystal X-ray diffraction analysis. A natural population analysis (NPA) performed on the B3LYP/ LANL2DZ level of theory for the molecular structures of the isoelectronic species [Ph$_2$Si(OSn$t$Bu$_2$)$_2$O·$t$Bu$_2$Sn(OH)$_2$] (**1**) and [Ph$_2$P(OSn$t$Bu$_2$)$_2$O·$t$Bu$_2$Sn(OH)$_2$]$^+$ (**6a**) suggests that the positive charge of the latter is partially delocalised over the phenyl rings.

(© Wiley-VCH Verlag GmbH & Co. KGaA, 69451 Weinheim, Germany, 2003)

## Introduction

In the last two decades there has been considerable interest in the chemistry of organotin−oxo clusters,[1] and particularly in those with Sn−O−P linkages.[1−8] In this regard, we and others have reported a variety of trinuclear organotin−oxo clusters [M(OSn$t$Bu$_2$)$_2$O·$t$Bu$_2$Sn(OH)$_2$] [M = Ph$_2$Si (**1**),[9] Me$_2$Si (**2**),[10] CO (**3**),[11] and MesB (**4**)[12]] and [Ph$_2$Si(OSn$t$Bu$_2$)$_2$O·$t$Bu$_2$SnF$_2$] (**5**)[13] that adopt a common tricyclic, almost planar ESn$_3$O$_3$X$_2$ (E = Si, C, B; X = OH, F) structural motif (Scheme 1). It was proposed that further examples of this class of compound might be accessible upon replacement of E by other organometallic fragments.[13]



1, M = Ph$_2$Si, X = OH
2, M = Me$_2$Si, X = OH
3, M = OC, X = OH
4, M = MesB, X = OH
5, M = Ph$_2$Si, X = F
6a, M = Ph$_2$P$^+$, X = OH
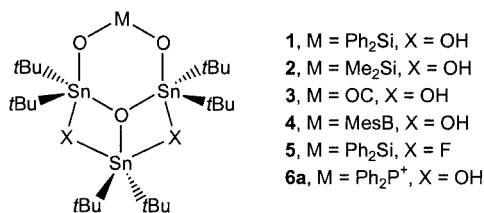
Scheme 1

[a] Centre for Chiral and Molecular Technologies, Deakin University,
Geelong 3217, Australia
Fax: (internat.) +61-3-5227-1040
E-mail: beckmann@deakin.edu.au

[b] Lehrstuhl für Anorganische Chemie II, Universität Dortmund,
44221 Dortmund, Germany.
Fax: (internat.) +49-231-7553800
E-mail: kjur@platon.chemie.uni-dortmund.de

We now describe the synthesis and structure of [Ph$_2$P(OSn$t$Bu$_2$)$_2$O·$t$Bu$_2$Sn(OH)$_2$](O$_3$SCF$_3$) (**6**), which features a cation, [Ph$_2$P(OSn$t$Bu$_2$)$_2$O·$t$Bu$_2$Sn(OH)$_2$]$^+$ (**6a**), that is isoelectronic to **1** and possesses a PSn$_3$O$_3$(OH)$_2$ structural motif in solution and in the solid state. The existence of the cation **6a** was recently suggested on the basis of a prominent mass cluster found in the electrospray mass spectrum of the eight-membered heterocycle *cyclo*-[Ph$_2$P(OSn$t$Bu$_2$O)$_2$PPh$_2$](O$_3$SCF$_3$)$_2$.[7]

## Results and Discussion

The consecutive reaction of di-*tert*-butyltin oxide with triflic acid and diphenylphosphinic acid provided the trinuclear organotin−oxo cluster [Ph$_2$P(OSn$t$Bu$_2$)$_2$O·$t$Bu$_2$Sn-(OH)$_2$](O$_3$SCF$_3$) (**6**) in good yield [Equation (1)].

$$(t\text{Bu}_2\text{SnO})_3 + \text{F}_3\text{CSO}_3\text{H} + \text{Ph}_2\text{PO}_2\text{H} \longrightarrow$$

$$[\text{Ph}_2\text{P(OSn}t\text{Bu}_2)_2\text{O}\cdot t\text{Bu}_2\text{Sn(OH)}_2](\text{O}_3\text{SCF}_3)$$
**6**

(1)
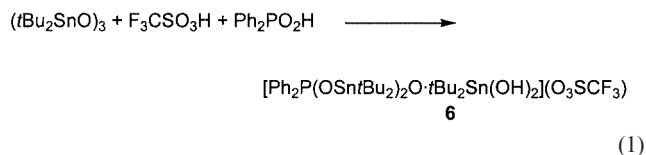
Compound **6** comprises air-stable colourless crystals that are readily soluble in most common organic solvents. The $^{119}$Sn NMR spectrum of **6** in [D$_3$]MeCN reveals a singlet at δ = −240.4 and a doublet at δ = −269.1 with a $^2J$($^{119}$Sn-O-$^{31}$P) coupling constant of 134 Hz, with an integral ratio of 1:2. The $^{119}$Sn chemical shifts are consistent with penta-coordinate tin atoms. The $^{119}$Sn NMR spectrum of **6** in

[D$_8$]toluene shows almost identical signals at $\delta = -243.3$ and $-271.9$ ppm [$^2J(^{119}$Sn-O-$^{31}$P) = 140 Hz], which apparently suggests that acetonitrile is not involved in strong coordination to the tin atoms. High temperature $^{119}$Sn NMR measurements ($T$ = 90 °C) in [D$_8$]toluene indicate the high configurative stability of **6**, which contrasts with the tendency of [Ph$_2$Si(OSn$t$Bu$_2$)$_2$O·$t$Bu$_2$Sn(OH)$_2$] (**1**) to undergo a reversible dissociation in chloroform into [Ph$_2$Si(OSn$t$Bu$_2$)$_2$O], ($t$Bu$_2$SnO)$_3$ and water, even at room temperature.[9] The $^{31}$P NMR spectrum of **6** in [D$_3$]MeCN shows a signal at $\delta$ = 33.1 ppm with unresolved tin satellites [$^2J(^{31}$P-O-$^{119/117}$Sn) = 136 Hz]. The electrospray mass spectrum (positive mode, cone voltage 20 V) of **6** displays two intense mass clusters at 965.2 and 700.1 Da that were unambiguously assigned to the organotin cations [Ph$_2$P(OSn$t$Bu$_2$)$_2$O·$t$Bu$_2$Sn(OH)$_2$]⁺ (**6a**) and [Ph$_2$P(OSn$t$Bu$_2$)$_2$O]⁺ (**6b**), respectively. A conductivity measurement (372 μS cm⁻¹; $c$ = 3.33 mmol·L⁻¹, $\Lambda$ = 112 S cm² mol⁻¹) of **6** confirms the electrolytic dissociation into **6a** and triflate anions in MeCN.[14]

## Solid-State Structure of [Ph$_2$P(OSn$t$Bu$_2$)$_2$O·$t$Bu$_2$Sn(OH)$_2$][O$_3$SCF$_3$] (6)

The molecular structure of [Ph$_2$P(OSn$t$Bu$_2$)$_2$O·$t$Bu$_2$Sn(OH)$_2$](O$_3$SCF$_3$) (**6**) is shown in Figure 1; selected bond lengths and angles are collected in Table 1. Like its closely related stannasiloxane derivatives [Ph$_2$Si(OSn$t$Bu$_2$)$_2$O·$t$Bu$_2$SnX$_2$] [X = OH (**1**),[9] F (**5**)[13]], the [PSn$_3$O$_3$(OH)$_2$] structural motif of **6a** is almost planar, the largest deviation from the plane being 0.033(3) Å. All three tin atoms show slightly distorted trigonal bipyramidal configurations [geometrical goodness[15] $\Delta\Sigma(\theta)$ = 89.0° for Sn(1), 89.6° for Sn(2), 90.1° for Sn(3)], in which two carbon

atoms and an oxygen atom occupy the equatorial positions [C(10), C(20) and O(1) for Sn(1); C(30), C(40) and O(1) for Sn(2); C(50), C(60) and O(1) for Sn(3)]. The axial positions are occupied by O(2) and O(4) for Sn(1), O(3) and O(5) for Sn(2), and O(4) and O(5) for Sn(3).

Table 1. Selected bond lengths [Å] and bond angles [°] for **6**; symmetry operation used to generate equivalent atoms: $a$ = $-x$, $y$ −1/2, −1/2 − $z$.

| | | | |
|---|---|---|---|
| Sn(1)−O(1) | 2.076(2) | Sn(1)−O(2) | 2.192(3) |
| Sn(1)−O(4) | 2.138(2) | Sn(1)−C(10) | 2.183(4) |
| Sn(1)−C(20) | 2.187(4) | Sn(2)−O(1) | 2.075(2) |
| Sn(2)−O(3) | 2.200(3) | Sn(2)−O(5) | 2.134(3) |
| Sn(2)−C(30) | 2.181(4) | Sn(2)−C(40) | 2.185(4) |
| Sn(3)−O(1) | 2.152(2) | Sn(3)−O(4) | 2.109(3) |
| Sn(3)−O(5) | 2.106(3) | Sn(3)−C(50) | 2.188(4) |
| Sn(3)−C(60) | 2.180(4) | P(1)−O(2) | 1.509(3) |
| P(1)−O(3) | 1.493(3) | P(1)−C(70) | 1.795(4) |
| P(1)−C(80) | 1.818(3) | O(4)−O(6) | 2.787(5) |
| O(5)−O(7a) | 2.786(5) | | |
| | | | |
| O(1)−Sn(1)−O(2) | 89.93(9) | O(1)−Sn(1)−O(4) | 72.53(9) |
| O(2)−Sn(1)−O(4) | 162.45(10) | O(1)−Sn(1)−C(10) | 117.27(12) |
| O(1)−Sn(1)−C(20) | 118.24(13) | O(2)−Sn(1)−C(10) | 90.67(13) |
| O(2)−Sn(1)−C(20) | 90.33(13) | O(4)−Sn(1)−C(10) | 96.83(13) |
| O(4)−Sn(1)−C(20) | 98.34(13) | C(20)−Sn(1)−C(10) | 124.48(16) |
| O(1)−Sn(2)−O(3) | 89.02(9) | O(1)−Sn(2)−O(5) | 72.61(10) |
| O(3)−Sn(2)−O(5) | 161.47(12) | O(1)−Sn(2)−C(30) | 117.26(12) |
| O(1)−Sn(2)−C(40) | 118.13(13) | O(3)−Sn(2)−C(30) | 91.81(16) |
| O(3)−Sn(2)−C(40) | 89.30(14) | O(5)−Sn(2)−C(30) | 98.87(16) |
| O(5)−Sn(2)−C(40) | 96.91(14) | C(30)−Sn(2)−C(40) | 124.69(16) |
| O(1)−Sn(3)−O(4) | 71.59(9) | O(1)−Sn(3)−O(5) | 71.66(10) |
| O(4)−Sn(3)−O(5) | 143.20(11) | O(1)−Sn(3)−C(50) | 119.97(13) |
| O(1)−Sn(3)−C(60) | 119.79(14) | O(4)−Sn(3)−C(50) | 101.03(14) |
| O(4)−Sn(3)−C(60) | 97.14(15) | O(5)−Sn(3)−C(50) | 98.77(14) |
| O(5)−Sn(3)−C(60) | 99.20(15) | C(50)−Sn(3)−C(60) | 120.24(16) |
| O(2)−P(1)−O(3) | 115.22(14) | O(2)−P(1)−C(70) | 108.52(18) |
| O(2)−P(1)−C(80) | 105.28(18) | O(3)−P(1)−C(70) | 110.30(19) |
| O(3)−P(1)−C(80) | 113.3(2) | C(70)−P(1)−C(80) | 103.40(18) |
| Sn(1)−O(1)−Sn(2) | 143.63(11) | Sn(1)−O(1)−Sn(3) | 108.29(9) |
| Sn(1)−O(4)−Sn(3) | 108.29(9) | Sn(2)−O(1)−Sn(3) | 108.07(10) |
| Sn(2)−O(5)−Sn(3) | 107.59(14) | Sn(1)−O(2)−P(1) | 140.30(16) |
| Sn(2)−O(3)−P(1) | 141.72(16) | | |

The effects of the variation of E and X upon the overall geometry of the tristannoxane motif of [Ph$_2$E(OSn$t$Bu$_2$)$_2$O·$t$Bu$_2$Sn(X)$_2$] [E = P⁺, X = OH (**6a**); E = Si, X = OH (**1**); E = Si, X = F (**5**)] is shown in Table 2 and can be summarized as follows: (*i*) The Sn(1)−O(1) and Sn(2)−O(1) distances show only marginal differences. The Sn(3)−O(1) distances decrease in the order **6 > 1 > 5**. (*ii*) The Sn(1)−X(1) and Sn(2)−X(2) distances increase on going from **6** to **1** and then **5**, which is consistent with the dissociation of compound **1** in solution, as shown by variable temperature $^{119}$Sn NMR spectroscopy.[9] (*iii*) The Sn(1)−O(2) and Sn(2)−O(3) distances also decrease in the order **6 > 1 > 5**. (*iv*) The geometrical goodness $\Delta\Sigma(\theta)$[15] of the trigonal bipyramidal configurations for Sn(1) and Sn(2), is best for compound **6**. For the Sn(3) atom there is almost no difference between compounds **1**, **5** and **6** .

Consistent with the $^{119}$Sn chemical shifts in solution and the molecular structure established by X-ray diffraction, the $^{119}$Sn MAS NMR spectrum of **6** shows two signals at $\delta$ =
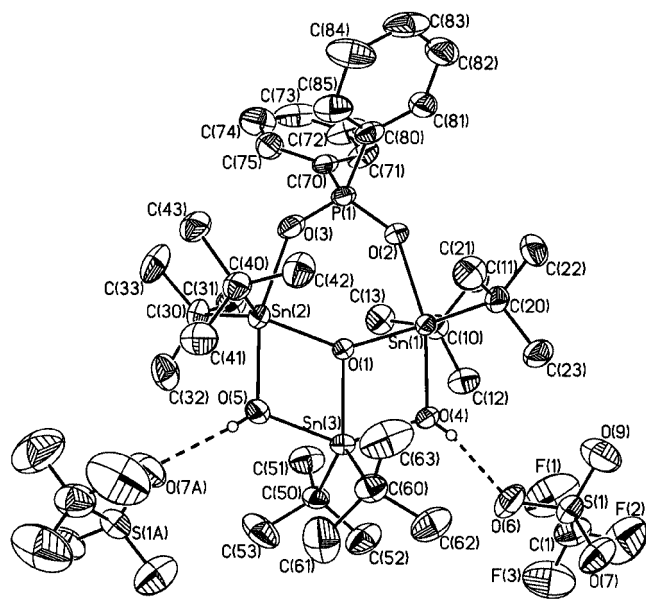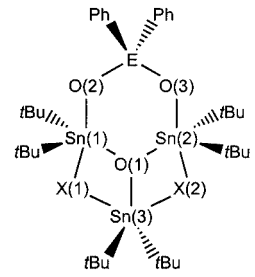


Figure 1. ORTEP diagram of the cation **6a** and two associated triflate anions showing 30% probability displacement ellipsoids and the atom numbering scheme (symmetry transformations used to generate equivalent atoms: $a$ = $-x$, $y$ −1/2, −1/2 − $z$)

Table 2. Comparison of selected bond lengths [Å] and geometrical goodness' [°]; [definition: $\Delta\Sigma(\theta) = \Sigma(\theta_{eq}) - \Sigma(\theta_{ax})$; 0°(tetrahedron) $\leq \Delta\Sigma(\theta) \leq$ 90°(trigonal bipyramid)][15] for **1**, **5** and **6a**

Ph    Ph
 \   /
  E
 /   \
O(2)   O(3)
tBu\\\         \\\\tBu
    Sn(1)    Sn(2)
tBu/    O(1)    \tBu
   X(1)      X(2)
      Sn(3)
     /    \
  tBu      tBu

**1**, E = Si, X = OH
**5**, E = Si, X = F
**6a**, E = P⁺, X = OH

| | **6a**, E = P⁺, X(1) = X(2) = O | **1**, E = Si,[9] X(1) = X(2) = O | **5**, E = Si,[13] X(1) = X(2) = F |
|---|---|---|---|
| Sn(1)−O(1) | 2.076(2) | 2.092(2) | 2.098(4) |
| Sn(2)−O(1) | 2.075(2) | 2.093(2) | 2.109(4) |
| Sn(3)−O(1) | 2.153(2) | 2.091(2) | 2.064(4) |
| Sn(1)−X(1) | 2.138(2) | 2.261(3) | 2.399(3) |
| Sn(3)−X(1) | 2.109(3) | 2.106(3) | 2.074(3) |
| Sn(2)−X(2) | 2.134(3) | 2.264(3) | 2.353(3) |
| Sn(3)−X(2) | 2.109(3) | 2.103(3) | 2.073(3) |
| Sn(1)−O(2) | 2.192(3) | 2.020(2) | 1.981(4) |
| Sn(2)−O(3) | 2.200(3) | 2.018(3) | 1.999(4) |
| $\Delta\Sigma(\theta)$ for Sn(1) | 89.0 | 73.7 | 65.9 |
| $\Delta\Sigma(\theta)$ for Sn(2) | 89.6 | 74.2 | 64.5 |
| $\Delta\Sigma(\theta)$ for Sn(3) | 90.1 | 89.7 | 88.2 |

−246.1 and −277.9 with an integral ratio of 39:61 and accompanying sets of spinning sidebands. The sets of spinning sidebands were used to perform a tensor analysis according to the method of Herzfeld and Berger;[16] the results are collected along with those of the stannasiloxane **1** in Table 3. In view of the similar molecular structures of compounds **1** and **6**, it is not surprising that the anisotropy ($\zeta$) and asymmetry ($\eta$) parameters are also comparable. With the data at hand, it appears that the anisotropy ($\zeta$) somewhat correlates with an increasing geometrical goodness $\Delta\Sigma(\theta)$; however, this tentative observation may be subject to revision when more examples are available for comparison. The individual P−O bond lengths of the organotin phosphinate **6** [1.493(3), 1.509(3) Å] differ only slightly.

Table 3. Selected ¹¹⁹Sn MAS NMR parameters for **1** and **6**.

| | $\delta_{iso}$ [ppm][a] | % | $\zeta$ [ppm] | $\eta$ | $\sigma_{11}$ [ppm] | $\sigma_{22}$ [ppm] | $\sigma_{33}$ [ppm] |
|---|---|---|---|---|---|---|---|
| **1**[9] | −265.7 | 33 | 471 | 0.61 | −115 | 175 | 737 |
| | −273.7 | 67 | 417 | 0.68 | −78 | 207 | 692 |
| **6** | −246.1 | 39 | 508 | 0.45 | −123 | 106 | 755 |
| | −277.9 | 61 | 522 | 0.60 | −140 | 174 | 800 |

[a] Definitions: $\delta_{iso} = -\sigma_{iso} = -(\sigma_{11} + \sigma_{22} + \sigma_{33})/3$; $\zeta = \sigma_{33} - \sigma_{iso}$ and $\eta = \sigma_{22} - \sigma_{11}/\sigma_{33} - \sigma_{iso}$ where $\sigma_{11}$, $\sigma_{22}$ and $\sigma_{33}$ are the principal tensor components on the shielding anisotropy (SA), sorted as follows $\sigma_{33} - \sigma_{iso} > \sigma_{11} - \sigma_{iso} > \sigma_{22} - \sigma_{iso}$.

In the crystal lattice, the cations **6a** are associated with the triflate anions through O(4)-H(4)···O(6) and O(5)-H(5)···O(7a) hydrogen bonds giving rise to the formation of an infinite chain (symmetry operation: $a = -x$, $y -1/2$, $-1/2 - z$), as shown in Figure 2. The O(4)···O(6) and O(5)···O(7a) distance of 2.789(6) and 2.791(6) Å, respectively, and the position of the corresponding OH stretching vibration ν(OH) at 3338 cm⁻¹ in the IR spectrum of **6** are indicative of medium-strength hydrogen bonding.[17] The fact that the triflate anions are not involved in coordination to tin atoms is also reflected by IR spectroscopy. Generally, for the free triflate anion ($C_{3v}$ symmetry) the asymmetric SO₃ stretching vibration $\nu_{as}(SO_3)$ is doubly degenerate, whereas in the presence of sufficiently large cation−anion interactions the axial symmetry is diminished ($C_s$ symmetry), and the asymmetric SO₃ stretching vibration $\nu_{as}(SO_3)$ splits into two components.[18] Thus, for [Ph₂P(OSn*t*Bu₂)₂O·*t*Bu₂Sn(OH)₂](O₃SCF₃) (**6**), the non-coordinating triflate anion gives rise to only one IR absorption (KBr) for the asymmetric SO₃ stretching vibration $\nu_{as}(SO_3)$ at 1285 cm⁻¹. The symmetric SO₃ stretching vibration $\nu_s(SO_3)$ is found at 1034 cm⁻¹.

**Charge Distribution in [Ph₂E(OSn*t*Bu₂)₂O·*t*Bu₂Sn(OH)₂] [E = Si (1), P⁺ (6a)]**

Considering the structural similarity of [Ph₂E(OSn*t*Bu₂)₂O·*t*Bu₂Sn(OH)₂] with E = Si (**1**) and E = P⁺ (**6a**), the question arises as to where the positive charge of **6a** is situated. In an effort to answer this question a natural population analysis (NPA)[19] was performed at the B3LYP/LANL2DZ level of theory and the atomic charges are given in Scheme 2. Somewhat unexpected, the atomic charges of the Si and P atoms are almost alike at about 2.2 (variation < 0.1). Moreover, the atomic charges of all Sn atoms are almost identical at about 2.5 for both compounds (variation < 0.05). However, this result is essentially in agreement with the results obtained by single-crystal X-ray structure determination. In compound **1** the Sn(1)−O(2) and Sn(2)−O(3) bond lengths of 2.020(2) and 2.018(3) Å, respectively, are somewhat shorter than the corresponding values of 2.192(3) and 2.200(3) Å in **6a**. The Sn−O bonding situation is reversed for the Sn(1)−X(1) and Sn(2)−X(2) bond lengths [2.261(3) and 2.264(3) Å in **1**; 2.138(2) and 2.134(3) Å in **6a**]. A minor difference of +0.26 is found for the atomic charges of the two E−O oxygen atoms (E = Si, P). A more significant change of +0.48 is observed for the group atomic charges of the two phenyl groups on going from **1** to **6a**. The remainder of the atomic charge difference of +0.24 is almost equally divided over the six *tert*-butyl groups (variation per *tert*-butyl group smaller than 0.05). Thus, it appears that the largest fraction of the positive charge in **6a** is delocalised over the polarisable phenyl groups. Apparently, this observation provides a reasonable explanation for the absence of strong cation−anion interactions in **6**, which is in marked contrast to the related eight-membered heterocycle *cyclo*-[Ph₂P(OSn*t*Bu₂O)₂PPh₂](O₃SCF₃)₂.[7]
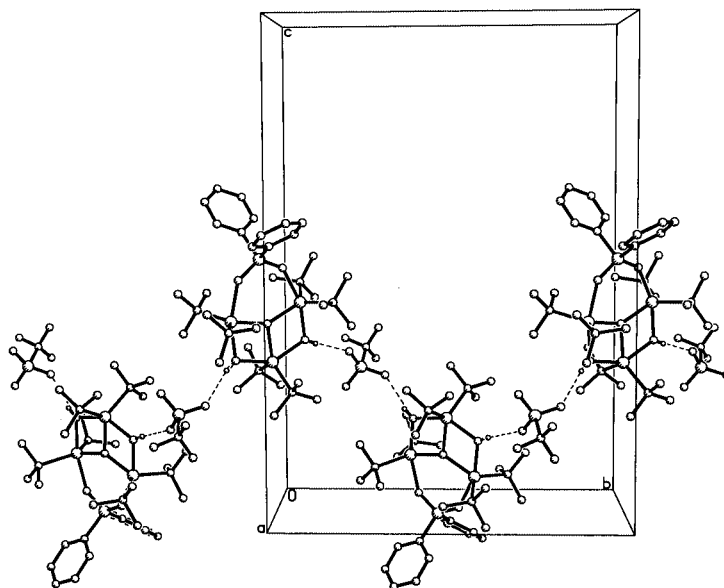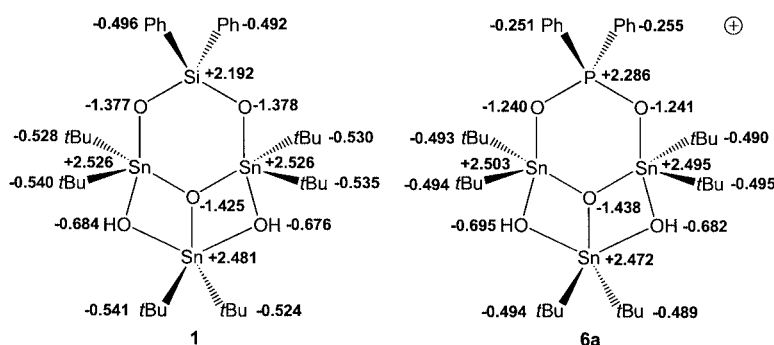
Figure 2. Perspective view through the *c*-axis of **6** showing the hydrogen bond interaction in the crystal lattice



Scheme 2

## Experimental Section

**General Remarks:** (*t*Bu$_2$SnO)$_3$ was prepared according to the literature.[20] F$_3$CSO$_3$H and Ph$_2$PO$_2$H were purchased from Aldrich. The solution NMR spectra (conc. 50 mg/300 μL; 25 °C) were measured using a Jeol Eclipse Plus 400 spectrometer [at 399.78 MHz ($^1$H) 100.54 ($^{13}$C) 161.84 ($^{31}$P) 149.05 ($^{119}$Sn)] and were referenced against SiMe$_4$, aqueous H$_3$PO$_4$ (90%) and SnMe$_4$. The solid-state NMR spectra were measured using the same instrument equipped with a 4 mm MAS probe. Crystalline NH$_4$H$_2$PO$_4$ (δ = 0.95 ppm) and *c*-Hex$_4$Sn (δ = −97.35 ppm) were used as secondary references. The $^{119}$Sn MAS NMR spectra were obtained using cross polarization (contact time 5 ms, recycle delay 10s). The isotropic chemical shifts δ$_{iso}$ were determined by comparison of two acquisitions measured at sufficiently different spinning frequencies. The tensor analyses were performed using the method of Herzfeld and Berger[16] implemented in DmFit 2002.[21] The IR spectrum was recorded using a BioRad FTIR spectrometer. The ESMS spectrum was obtained with a Platform II single quadrupole mass spectrometer (Micromass, Altrincham, UK) using an acetonitrile mobile phase. MeCN solutions (0.1 mM) were injected directly into the spectrometer with a Rheodyne injector equipped with a 50 μL loop. A Harvard 22 syringe pump delivered the solutions to the vaporis-

ation nozzle of the electrospray ion source at a flow rate of 10 μL min$^{-1}$. Nitrogen was used both as a drying gas and for nebulization with flow rates of approx. 200 mL min$^{-1}$ and 20 mL min$^{-1}$ respectively. The pressure in the mass analyser region was usually about 4 × 10$^{-5}$ mbar. The conductivity measurement was performed using a CDM80 Conductivity Meter equipped with a CDC104 Conductivity Cell (Radiometer Copenhagen, DK) at 25 °C. Microanalysis was carried out by CMAS, Belmont, Australia.

**[Ph$_2$P(OSn*t*Bu$_2$)$_2$O·*t*Bu$_2$Sn(OH)$_2$](O$_3$SCF$_3$) (6):** F$_3$CSO$_3$H (150 mg, 1.00 mmol) was added to a suspension of (*t*Bu$_2$SnO)$_3$ (747 mg, 1.00 mmol) in MeCN (20 mL) whilst stirring at room temperature. After 10 min, solid Ph$_2$PO$_2$H (218 mg, 1.00 mmol) was added, and the mixture heated at 85 °C for 12 h. The solvent was removed in vacuo, to yield a white powder, which was recrystallized from CHCl$_3$/MeCN to give colourless crystals of **6** [959 mg, 0.86 mmol, 86%; m.p. 220 °C (dec)].

$^{119}$Sn NMR ([D$_3$]MeCN): δ = −240.4 (1Sn), −269.1 [d, 2Sn; $^2J$($^{119}$Sn-O-$^{31}$P) = 134 Hz] ppm. $^{119}$Sn NMR ([D$_8$]toluene): δ = −243.3 (1Sn), −271.9 [d, 2Sn; $^2J$($^{119}$Sn-O-$^{31}$P) = 140 Hz] ppm. $^{31}$P NMR ([D$_3$]MeCN): δ = 33.1 [$^2J$($^{31}$P-O-$^{119/117}$Sn) = 136 Hz] ppm. $^{13}$C NMR ([D$_3$]MeCN): δ = 133.0, 131.0, 129.9, 127.4, 119.2, 41.8, 38.9, 28.7, 28.5 ppm. $^1$H NMR ([D$_3$]MeCN): δ = 8.00−7.50 (m,

10 H), 1.52 (s, 9 H, $^3J(^1$H-$^{119}$Sn) = 112 Hz), 1.48 (s, 18 H, $^3J(^1$H-$^{119}$Sn) = 119 Hz) ppm. $^{119}$Sn MAS NMR: δ = −246.1 (1 Sn), −277.9 (2 Sn) ppm. $^{31}$P MAS NMR: δ = 27.4 ppm. IR (KBr): ṽ = 3338 br, 3064 w, 2976 m, 2947 m, 2853 s, 1466 m, 1441 w, 1396 w, 1366 w, 1285 s, 1253 s, 1224 w, 1166 s, 1131 vs, 1048 s, 1034 m, 1014 m, 998 w, 941 w, 802 w, 756 w, 721 m, 698 w, 665 w, 638 m, 548 m, 532 m, 448 m cm$^{-1}$. $C_{37}H_{66}F_3O_8PSSn_3$ (1115.16): calcd. C 39.85, H, 5.97; found C 39.82, H 6.00. ES MS (positive mode, cone voltage 20 V): $m/z$ = 700.1 $[Ph_2P(OSntBu_2)_2O]^+$, 965.2 $[Ph_2P(OSntBu_2)_2O·tBu_2Sn(OH)_2]^+$. Conductivity measurement (MeCN; $c$ = 3.33 mmol·L$^{-1}$): 372 μS cm$^{-1}$.

**X-ray Crystallographic Study:** Single crystals of $[Ph_2P(OSntBu_2)_2O·tBu_2Sn(OH)_2](O_3SCF_3)$ (**6**) suitable for X-ray crystallography were obtained by slow evaporation of a $CH_2Cl_2$/$n$-hexane solution. Data and structure solution at $T$ = 293(2) K: $C_{37}H_{66}F_3O_8PSSn_3$, (1115.00), orthorhombic, $P2_12_12_1$, crystal dimensions: 0.20 × 0.25 × 0.45 mm$^3$, $a$ = 10.7376(6), $b$ = 17.9769(10), $c$ = 25.4598(14) Å, $V$ = 4914.5(5) Å$^3$, $Z$ = 4, $\rho_{calcd.}$ = 1.507 Mg·m$^{-3}$, $F(000)$ = 2240, $\mu$ = 1.640 mm$^{-1}$. Intensity data were collected on a Bruker SMART Apex CCD diffractometer fitted with Mo-$K_\alpha$ radiation (graphite crystal monochromator, λ = 0.71073 Å) to a maximum of $\theta_{max}$ = 27.52° via ω scans (completeness 99.6% to $\theta_{max}$). Data were reduced and corrected for absorption using the programs SAINT and SADABS.[22] The structure was solved by direct methods and difference Fourier synthesis using SHELX-97 implemented in the program WinGX 2002.[23] Full-matrix least-squares refinement on $F^2$ using all data was carried out with anisotropic displacement parameters applied to all non-hydrogen atoms. The hydrogen atoms H(4) and H(5) were located in the Fourier density map and refined isotropically, whereas all other hydrogen atoms were included in geometrically calculated positions using a riding model and were refined isotropically. One phenyl group is disordered over two positions with occupancies of 0.8 [C(80) to C(85)] and 0.2 [C(80′) to C(85′)], which were refined as regular hexagons (AFIX66). One carbon atom of a *tert*-butyl group is also disordered and was refined over two sites with occupancies of 0.7 C(61) and 0.3 C(61′). The weighting scheme employed was of the type $w$ = $[\sigma^2(F_o^2) + (0.0404\ P)^2 + 0.6740\ P]^{-1}$ where $P$ = $(F_o^2 + 2\ F_c^2)/3$. $R_1$ = 0.0284 for 10422 $[I > 2\sigma(I)]$ reflections and $wR_2$ = 0.0692 for 11216 independent reflections; GooF = 1.035. The Flack parameter was −0.002(17).[24] The max. and min. residual electron densities were 0.900/−0.233 e·Å$^{-3}$. CCDC-213484 contains the supplementary crystallographic data for this paper. These data can be obtained free of charge at www.ccdc.cam.ac.uk/ conts/retrieving.html [or from the Cambridge Crystallographic Data Centre, 12, Union Road, Cambridge CB2 1EZ, UK; Fax: (internat.) +44-1223-336-033; E-mail: deposit@ccdc.cam.ac.uk].

**MO Calculation:** Single point calculations based on the coordinates of the molecular structures of $[Ph_2E(OSntBu_2)_2O·tBu_2Sn(OH)_2]$ with E = Si (**1**) and E = P$^+$ (**6a**) were performed at the B3LYP/ LANL2DZ level of theory using Gaussian 98.[25] Natural bond orbital charges were obtained using NBO 5.0.[26]

## Acknowledgments

[1] V. Chandrasekhar, S. Nagendran, V. Baskar, *Coord. Chem. Rev.* **2002**, *235*, 1−52.
[2] R. R. Holmes, *Acc. Chem. Res.* **1989**, *22*, 190−197.
[3] V. K. Jain, *Coord. Chem. Rev.* **1994**, *135/136*, 809−843.
[4] F. Ribot, C. Sanchez, M. Biesemans, F. A. G. Mercier, J. C. Martins, M. Gielen, R. Willem, *Organometallics* **2001**, *20*, 2593−2603.
[5] A. F. Shihada, F. Weller, *Z. Anorg. Allg. Chem.* **2001**, *627*, 638−644.
[6] V. Chandrasekhar, V. Baskar, A. Steiner, S. Zacchini, *Organometallics* **2002**, *21*, 4528−4532.
[7] J. Beckmann, D. Dakternieks, A. Duthie, C. Mitchell, *Organometallics* **2003**, *22*, 2161−2164.
[8] J. Beckmann, D. Dakternieks, A. Duthie, C. Mitchell, *Dalton Trans.* **2003**, 3258−3263.
[9] J. Beckmann, K. Jurkschat, B. Mahieu, M. Schürmann, *Main Group Met. Chem.* **1998**, *21*, 113−122.
[10] F. Cervantes-Lee, H. K. Sharma, I. Haiduc, K. H. Pannell, *J. Chem. Soc., Dalton Trans.* **1998**, 1−2.
[11] H. Reuter, PhD thesis, University of Bonn, Germany, **1986**.
[12] P. Brown, M. F. Mahon, K. C. Molloy, *J. Chem. Soc., Dalton Trans.* **1992**, 3503−3509.
[13] J. Beckmann, K. Jurkschat, M. Schürmann, D. Suter, R. Willem, *Organometallics* **2002**, *21*, 3819−3822.
[14] W. J. Geary, *Coord. Chem. Rev.* **1971**, *7*, 81−122.
[15] U. Kolb, M. Beuter, M. Dräger, *Inorg. Chem.* **1994**, *33*, 4522−4530.
[16] J. Herzfeld, X. Chen *Encyclopedia of Nuclear Magnetic Resonance, Vol. 7*, Eds.; D. M. Grant, R. K. Harris, John Wiley & Sons, Chichester, **1996**, 6021−6030.
[17] G. A. Jeffrey, *An Introduction to Hydrogen Bonding*, Oxford University Press, New York, **1997**.
[18] G. A. Lawrance, *Chem. Rev.* **1986**, *86*, 17−33.
[19] A. E. Reed, L. A. Curtiss, F. Weinhold, *Chem. Rev.* **1988**, *88*, 899−926.
[20] H. Puff, W. Schuh, R. Sievers, W. Wald, R. Zimmer, *J. Organomet. Chem.* **1984**, *260*, 271−280.
[21] D. Massiot, F. Fayon, M. Capron, I. King, S. Le Calvé, B. Alonso, J.-O. Durand, B. Bujoli, Z. Gan, G. Hoatson, *Mag. Res. Chem.* **2002**, *40*, 70−76.
[22] SMART, SAINT and SADABS, Siemens Analytical X-ray Instruments Inc. Madison, Wisconsin USA, **1999**.
[23] L. J. Farrugia, *J. Appl. Crystallogr.* **1997**, *20*, 565.
[24] H. D. Flack, *Acta Crystallogr., Sect. A* **1983**, *39* 876−881.
[25] Gaussian 98, Revision A.7, M. J. Frisch, G. W. Trucks, H. B. Schlegel, G. E. Scuseria, M. A. Robb, J. R. Cheeseman, V. G. Zakrzewski, J. A. Montgomery, R. E. Stratmann, J. C. Burant, S. Dapprich, J. M. Millam, A. D. Daniels, K. N. Kudin, M. C. Strain, O. Farkas, J. Tomasi, V. Barone, M. Cossi, R. Cammi, B. Mennucci, C. Pomelli, C. Adamo, S. Clifford, J. Ochterski, G. A. Petersson, P. Y. Ayala, Q. Cui, K. Morokuma, D. K. Malick, A. D. Rabuck, K. Raghavachari, J. B. Foresman, J. Cioslowski, J. V. Ortiz, B. B. Stefanov, G. Liu, A. Liashenko, P. Piskorz, I. Komaromi, R. Gomperts, R. L. Martin, D. J. Fox, T. Keith, M. A. Al-Laham, C. Y. Peng, A. Nanayakkara, C. Gonzalez, M. Challachombe, P. M. W. Gill, B. G. Johnson, W. Chen, M. W. Wong, J. L. Andres, M. Head-Gordon, E. S. Replogle, J. A. Pople, Gaussian, Inc., Pittsburgh, **1998**.
[26] NBO 5.0. E. D. Glendening, J. K. Badenhoop, A. E. Reed, J. E. Carpenter, J. A. Bohmann, C. M. Morales, F. Weinhold (Theoretical Chemistry Institute, University of Wisconsin, Madison, WI, **2001**.